JOURNAL OF SOLID STATE CHEMISTRY 72, 338–352 (1988)

Preparation and Crystal Structures of Plutonium(IV) Hexachloro Complexes, Rb_2PuCl_6 and K_2PuCl_6*

LESTER R. MORSS AND TAKEO FUJINO†

Chemistry Division, Argonne National Laboratory, 9700 South Cass Avenue, Argonne, Illinois 60439

Received December 8, 1986; in revised form June 3, 1987

Rb_2PuCl_6 and K_2PuCl_6 were prepared by heating mixtures of anhydrous $PuCl_3$ and the respective alkali metal chlorides under high Cl_2 pressures. Their crystal structures were determined by powder X-ray crystallography. Rb_2PuCl_6: hexagonal, space group $P6_3mc$, $a = 7.377 \pm 0.002$, $c = 11.880 \pm 0.007$ Å, $Z = 2$, $V = 279.9 \pm 0.3$ Å^3 (per formula), $D_x = 3.69$ g/cm^3. K_2PuCl_6: monoclinic, space group $P2/m$, $a = 7.218 \pm 0.005$, $b = 7.611 \pm 0.006$, $c = 10.208 \pm 0.007$ Å, $\beta = 91.59 \pm 0.04°$, $Z = 2$, $V = 280.3 \pm 0.3$ Å^3 (per formula), $D_x = 3.14$ g/cm^3. The variable atom parameters were obtained by means of electrostatic calculation to have the maximum Madelung constant. Raman spectra showed two lines corresponding to $\nu_1(A_{1g})$ and $\nu_5(F_{2g})$ for both compounds. The difference of stability in M_2PuCl_6 (M = K, Rb, Cs) is discussed.

Introduction

Studies to prepare and characterize actinide(IV) hexahalogeno complexes, $M_2^+An^{4+}X_6^-$, where M^+, An^{4+}, and X^- denote alkali metal, actinide(IV), and halogen ions, respectively, have been carried out for a variety of actinide elements. An interesting feature of these compounds is that they crystallize in several different crystal structures. The α-phase structure which is seen in α-Na_2ThF_6, α-K_2ThF_6, α-Na_2UF_6, and α-K_2UF_6 is cubic with space group $Fm3m$. These compounds are formed by quenching from the melt or by rapid precipitation from solution. In the crystals, the alkali metal and the actinide(IV) ions are randomly distributed over the metal sites of the fluorite structure (*1*).

The β_1 phase which appears in β_1-K_2ThF_6 (*2*), β_1-K_2UF_6 (*3, 4*), and presumably Rb_2ThF_6 (*5*) has a hexagonal structure with space group $C\bar{6}2m$-D_{3h}^3. In this structure, the basal faces of the trigonal prisms are shared by the polyhedra along the chains. The An^{4+} chains are crosslinked by the M^+–F^- bonding where each M^+ is at the center of $9F^-$ and the M^+–$9F^-$ polyhedra share edges with the An^{4+}–$9F^-$ polyhedra.

The β_2-type structure of β_2-Na_2ThF_6, β_2-Na_2UF_6, β_2-K_2UF_6 (*1, 2*), β_2-Na_2NpF_6 (*6*), and β_2-Na_2PuF_6 (*7*) is hexagonal, but their space group is $C32$-D_3^2. The actinide is coordinated by nine fluorines and the alkali metal by six fluorines. δ-Na_2UF_6 is reported

---

* The U.S. Government's right to retain a nonexclusive royalty-free license in and to the copyright covering this paper, for governmental purposes, is acknowledged.

† Present address: Division of Chemistry, Japan Atomic Energy Research Institute, Tokai-mura, Ibaraki 319-11, Japan.

0022-4596/88 $3.00

to crystallize in a somewhat different manner. This compound is hexagonal with $P3$, $Z = 2$ (*5*), where some of the sodium ions are found in polyhedra identical to that of uranium, i.e., at the centers of tricapped trigonal prisms.

There have also been orthorhombic structures reported. The space group for γ-Na_2UF_6 is $Immm$-D_{2h}^{25}, where the coordination number of fluorines around a sodium or uranium is 8, and the distances of Na^+–F^- and U^{4+}–F^- bonds are both 2.38 Å (*8*). On the other hand, Rb_2UF_6 is orthorhombic with space group $Cmcm$, $Z = 4$ (*9*). This structure is the K_2ZrF_6 type and consists of infinite chains of UF_8 polyhedra which can be described as dodecahedra with triangular faces. Rb_2NpF_6, Rb_2PuF_6, Rb_2AmF_6, and Rb_2CmF_6 have been reported to have the same structure (*10*).

Studies on hexachloro complexes are fewer. However, a characteristic feature of the reported structures is that the chloride compounds tend to crystallize in the trigonal or hexagonal system with space group $P\bar{3}m1$ or $P6_3mc$. Rb_2UCl_6 (*11*), α-Cs_2UCl_6 (*12, 13*), and Cs_2PuCl_6 (*12, 14*) have $P\bar{3}m1$, β-$(NH_4)_2SiF_6$-type structure. Cs_2BkCl_6 (*15*) and presumably β-Cs_2UCl_6 (*16*) have space group $P6_3mc$ with β-Rb_2GeF_6-type structure. The former type of compound has layers (perpendicular to c axis) with each layer consisting of $AnCl_6^{2-}$ groups with alkali metal ions approximately in the planes of lower and upper chlorides. The latter doubles the c axis, with alternate layers rotated 180° about sixfold screw axes.

There appear to be no structural studies of K_2UCl_6. According to a recent study by Bendall *et al.* (*17*), Na_2UCl_6 crystallizes in space group $P\bar{3}m1$ but in a different atomic arrangement ($Z = 3$, Na_2SiF_6 type) from Rb_2UCl_6, α-Cs_2UCl_6, or Cs_2PuCl_6 for which Z is 1. They also report that the best description of Li_2UCl_6 is a hexagonal cell, $P6_3/mmc$ and $Z = 3$, with uranium and lithium atoms disordered over the available octahedral sites. These results suggest that the crystallographic nature of the hexachloro complexes is considerably different from that of hexafluoro complexes.

Under these circumstances, it seemed very desirable to have more information about $M_2^+An^{4+}Cl_6$ compounds, especially of plutonium, because only the structure of Cs_2PuCl_6 has been clarified so far. We report here the preparation and the crystal structures of Rb_2PuCl_6 and K_2PuCl_6. The variable atom parameters of these structures were determined from electrostatic calculations (*18*). The chemical bonding and coordination of atoms are discussed with the aid of Raman spectra analysis.

Experimental

1. Materials Used

RbCl and KCl used were both of analytical grade. The isotopic ratio of plutonium metal used had been measured mass spectrometrically in June 1974 to be $^{238}Pu = 0.00083$, $^{239}Pu = 99.2589$, $^{240}Pu = 0.7309$, $^{241}Pu = 0.0091$, and $^{242}Pu < 0.001$ wt%. The stock solution of plutonium was obtained by dissolving a weighed sample of metal in 8 *M* HNO_3 and weighing the solution.

2. Preparation of the Complex Chlorides

The compound Rb_2PuCl_6 was prepared as follows: An aliquot of plutonium solution containing ca. 50 mg Pu was pipetted out of the stock solution and weighed precisely to determine the plutonium amount. All that solution was transferred to a cone by washing with dil HCl. Concentrated NH_4OH solution was added, and the plutonium hydroxide precipitate formed was centrifuged. The precipitate was dissolved with concd HCl. The procedure above was repeated twice in order to remove NO_3^- ion. To the HCl solution of plutonium, the solution containing the calculated amount of RbCl (Rb : Pu = 2 : 1) was added. After drying under an infrared lamp, the solid was transferred into a one-end sealed Pyrex tube for dehydration. Dehydration of the chlorides was carried out in an atmosphere of HCl gas at ca. 0.5 atm. The chloride mixture was first heated gradually to 120°C and then evacuated. Dry HCl gas was reintroduced, and the temperature was slowly raised to 300°C. The system was evacuated, and the sample was subsequently heated in HCl gas at ~350°C overnight. The dried solid was finely ground in an agate mortar and transferred into a quartz tube with evacuation fitting and rounded bottom. This was done in a dry-box filled with purified N_2.

After attachment to a vacuum line, the tube was evacuated, followed by an introduction of Cl_2 gas. The amount of the Cl_2 in the tube was adjusted so that the pressure would be ca. 50 atm at 400°C with no reaction. The tube was sealed off with a torch while cooling the bottom of the tube with liquid nitrogen. The amount of Cl_2 consumed by the reaction was calculated to be less than 10% of the total Cl_2 amount. The tube was put into an autoclave and the temperature was gradually raised up to 350°C.

After holding at that temperature for 4 days, the autoclave was slowly cooled to room temperature in 2 days. The Rb_2PuCl_6 obtained showed a pale yellow color.

The method of preparation of K_2PuCl_6 was the same as that for Rb_2PuCl_6 except that KCl was used instead of RbCl. The color of the product, K_2PuCl_6, was pale yellow.

3. *Analyses*

α-Assay of plutonium isotopes and ^{241}Am (daughter of ^{241}Pu) was made either by a conventional 2π counter or a low geometry counter in flowing PR gas atmosphere. The oxidation state of plutonium in the products was determined by visible and near-infrared spectra with a Cary 14 spectrophotometer after dissolving the samples in 1 *M* $HClO_4$ (*19*).

Raman spectra measurements were performed with a Spex 1403 spectrometer for the samples in glass capillaries. An exciting line of 5145 Å was used. Other conditions: laser power = 100 mW, int. time = 1 sec, and increment = 0.5 cm^{-1}.

4. *X-ray Diffraction Measurements*

X-ray powder diffraction photographs were taken with a 57.3-mm-diameter Debye–Scherrer camera using Ni-filtered Cu$K\alpha$ radiation.

High-resolution diffraction lines from as low as $2\theta = 10°$ were obtained for the specimens in capillaries with a Guinier–Simon focusing camera using curved quartz monochromatized Cu$K\alpha$ radiation. The diffraction angles were corrected with the reflections of an NBS Si standard sample. The relationship of 2θ and the length from origin in the films was proportional at least up to 80° (2θ).

Results

1. *Composition of the Compounds*

About 20 mg of the reaction product was precisely weighed and dissolved into ca. 5 ml 1 *M* $HClO_4$. After the weight of the solution was measured, an aliquot of ca. 20 mg solution was weighed out of it, which was then diluted with ca. 1 ml of 1 *M* $HClO_4$. A precisely weighed amount of the diluted solution (ca. 50 mg) was transferred onto a counting plate and subsequently heated to dryness and fixed to the plate by flaming. α-Radioactivity measurements showed that the plutonium amount in the rubidium compound was 37.6 wt%, which were in good agreement with the theoretical value, 38.4%, calculated for Rb_2PuCl_6. For the potassium compound, the plutonium amount from the α-radioassay was 42.9 wt% (theoretical value, 45.1 wt%, for K_2PuCl_6). The slightly smaller experimental values may be attributable to the shielding of the α-activities by the alkali metal atoms.

Visible and near-infrared spectra were

taken after dissolving the specimens in 1 *M* $HClO_4$ at 25°C. Both the Rb_2PuCl_6 and K_2PuCl_6 spectra showed a broad absorption band with a peak at 1075 nm, and a broad band with the maximum at 813 nm accompanied by two shoulders at 857 and 890 nm, and another very broad band with maximum around 730 nm. The spectra exhibited a very sharp peak at 471 nm in the visible region. These patterns are in good agreement with the Pu(IV) spectra in the literature (*19*). The relative concentrations of Pu(III), Pu(IV), Pu(V), and Pu(VI) were calculated using the characteristic peaks at 600, 471, 570, and 831 nm with molar extinction coefficients of 37, 56, 19, and 550, respectively. For the rubidium compound, the relative concentrations were Pu(III) = 3.4, Pu(IV) = 94.3, Pu(V) = 0.0, and Pu(VI) = 2.3%, and for the potassium compound, Pu(III) = 3.2, Pu(IV) = 95.9, Pu(V) = 0.0, and Pu(VI) = 0.9%. Existence of small amounts of Pu(III) and Pu(VI) is probably due to disproportionation of Pu(IV) in the solution. The results above for the Pu amounts and oxidation states in the products indicate that the compositions were Rb_2PuCl_6 and K_2PuCl_6.

2. *Determination of Structure*

Inspection of the Debye–Scherrer patterns of Rb_2PuCl_6 revealed that the crystal structure is the same as that of Cs_2BkCl_6 (*15*), i.e., hexagonal, space group $P6_3mc$, and isostructural with β-Rb_2GeF_6. Precise diffraction angle data, some of which were very close to each other, were collected as separated lines from the Guinier films. Unit cell dimensions were obtained using these data by least-squares calculations on a FACOM M-380. All observed lines could be indexed and these followed the general rule of the space group $P6_3mc$ that $l = 2n$ for *hhl* reflections. Program LCR-2 (*20*) weights each line proportional to $[\sin^2(2\theta)\sigma^2(\theta)]^{-1}$ where $\sigma(\theta)$ is the estimated error of a line reading. As the $\sigma(\theta)$ values, $\sigma(\theta) = \pm 0.05°$ was used for sharp lines, and ±0.1° for broad and/or very weak lines. The crystal data are shown in Table I. The observed and calculated $Q(=1/d^2)$ values are tabulated in Table II for each of the (*hkl*) reflections.

TABLE I

CRYSTAL DATA FOR Rb_2PuCl_6 AND K_2PuCl_6

	Rb_2PuCl_6	K_2PuCl_6
Crystal system:	Hexagonal	Monoclinic
Space group:	$P6_3mc$	$P2/m$
Z	2	2
a (Å)	7.377 ± 0.002	7.218 ± 0.005
b (Å)		7.611 ± 0.006
c (Å)	11.880 ± 0.007	10.208 ± 0.007
β (°)		91.59 ± 0.04
Cell volume (Å^3) (per formula)	279.9 ± 0.3	280.3 ± 0.3
X-ray density (g/cm^3)	3.69	3.14

Since acquisition of intensity data precise enough to work out atom positions is difficult from the films of Guinier–Simon camera, and since the present compounds are basically ionic, the variable atom positions were determined by an electrostatic method (*18*). The method comprises maximization (condition 1) of the Madelung constant for atom parameter variables under the restriction (condition 2) that the ion–ion separations of any pairs of ions are larger than the respective critical distances. The Madelung constants were computed using the method of Bertaut (*21*, *22*). The correctness of the program was checked by comparing the computed constants for several crystal structures with those of Johnson and Templeton (*23*). Another check was made by doing the calculation of CsCl constants with six different descriptions (*18*). Calculation for search of the maximum constants was performed for *h*, *k*, and *l*'s from −12 to 12 for prompt start of execution in the computer since the errors in the Madelung constants were systematic and they would not change the atom parameter values. However, the Madelung constants for finally obtained atom parameters are

TABLE II

OBSERVED AND CALCULATED Q VALUES AND INTENSITIES FOR Rb_2PuCl_6

(hkl)	Q(obs)[a]	Q(calc)	I(obs)[b]	I(calc)
100	0.0248	0.0245	6	1.1
002	0.0287	0.0283	7	2.5
101	0.0320	0.0316	10	10
102	0.0533	0.0528	7	3.3
110	0.0740	0.0735	9	6.7
103	0.0889	0.0883	8	6.0
112 201	0.1025	0.1018 0.1051	6	2.9 1.4
004	0.1140	0.1134	<1	0.5
202	0.1270	0.1263	8	7.3
104	0.1387	0.1379	2	1.2
203	0.1627	0.1618	7	4.5
210	0.1724	0.1715	1	0.6
211	0.1794	0.1786	4	2.6
114	0.1879	0.1869	2	0.8
212	0.2010	0.1999	3	2.0
105	0.2025	0.2016	4	1.7
204	0.2121	0.2114	2	1.4
300	0.2215	0.2205	3	1.6
213	0.2362	0.2353	5	3.2
302	0.2496	0.2489	3	0.9
205	0.2764	0.2752	4	2.4
214	0.2855	0.2849	2	0.5
220	0.2950	0.2940	5	3.5
222 311	0.3234	0.3224 0.3256	2	0.7 0.9
116	0.3297	0.3286	2	1.9
312 215	0.3500	0.3468 0.3486	3b	0.7 1.3
206	0.3539	0.3531	2	0.6
313	0.3831	0.3823	2	1.8
402	0.4211	0.4203	1	1.2
008 403	0.4574	0.4535 0.4558	1b	0.4 1.0
321	—	0.4726	—	0.6
306	—	0.4756	—	1.2
322 315	0.4970	0.4938 0.4957	1	0.3 1.2
410 217	0.5155	0.5145 0.5187	1	1.2 0.3
118 323	0.5295	0.5270 0.5293	1b	0.7 1.2
412	0.5435	0.5429	<1	0.7

[a] $Q = 1/d^2$ in $Å^{-2}$.

[b] Visually estimated.

those calculated in the range −18 to 18, where the magnitude of vector **h**(h, k, l) extends in reciprocal space to 5.11 and 3.46 $Å^{-1}$ for Rb_2PuCl_6 and K_2PuCl_6, respectively, lowering the errors in the constants down to the order of 10^{-5}.

In the crystal of Rb_2PuCl_6, there are seven variable atom parameters to be determined, i.e., u(Rb1), u(Rb2), u(Pu), u(Cl1), v(Cl1), u(Cl2), and v(Cl2), but all the atoms have the variable parameters along the c axis. Therefore, one of such parameters can be arbitrarily chosen (*15*). Here, u(Pu) was taken to be 0.25 in order to be consistent with the literature values (*12*). The symmetry relations of these parameters are given in Table III.

Figures 1a and 1b show a perspective and a side view of this crystal structure obtained by ORTEP2 program, respectively. As seen from these figures, each plutonium atom is coordinated by 6 chlorine atoms which form an octahedron, and each rubidium atom has 12 nearest neighbor chlorine atoms.

It has been shown in the preceding paper (*18*) that the Madelung constant changes with the following factors listed in order of decreasing magnitude:

(1) Contribution of coulombic attractive interaction between a cation with higher valency and anions coordinated around it is the largest.

(2) The interaction between a lower valency cation and the anions surrounding it is the next largest.

(3) There exists coulombic repulsion between anions, but this should be generally smaller than the above two due to longer

TABLE III

ATOM POSITIONS IN Rb_2PuCl_6 (SPACE GROUP $P6_3mc$)

Rb1:	(2b)	$\frac{1}{3}, \frac{2}{3}, u; \frac{2}{3}, \frac{1}{3}, u + \frac{1}{2}$ with $u = 0.8805$
Rb2:	(2a)	$0, 0, u; 0, 0, u + \frac{1}{2}$ with $u = 0.5943$
Pu:	(2b)	with $u = \frac{1}{4}$
Cl1:	(6c)	$u, \bar{u}, v; u, 2u, v; 2\bar{u}, \bar{u}, v;$ $\bar{u}, u, v + \frac{1}{2}; \bar{u}, 2\bar{u}, v + \frac{1}{2}; 2u, u, v + \frac{1}{2}$ with $u = 0.1464$, $v = 0.3523$
Cl2:	(6c)	with $u = 0.4972$, $v = 0.1092$

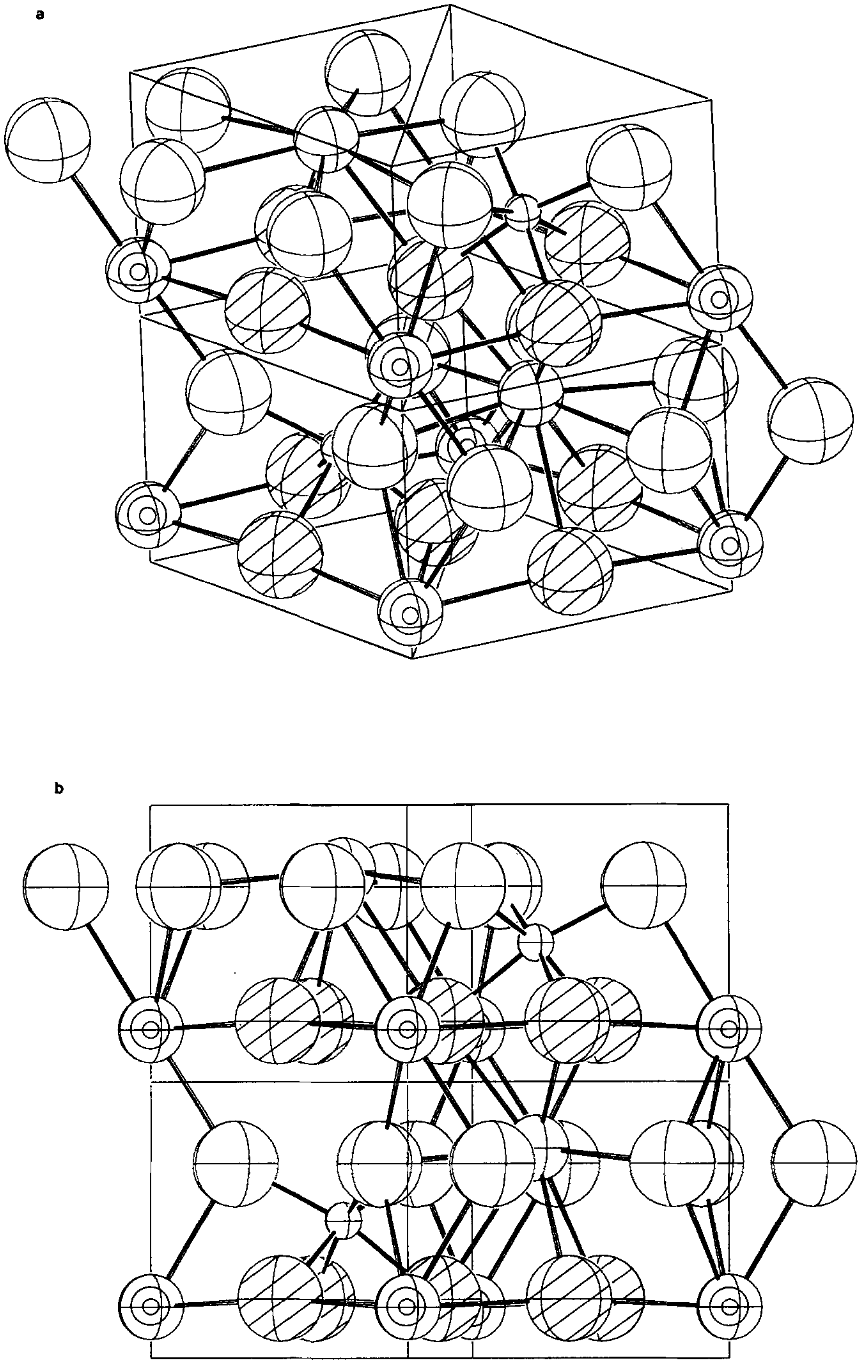

FIG. 1. Atom arrangement in Rb_2PuCl_6. (a) Perspective view; (b) side view. Smallest spheres, Pu; middle-sized spheres, Rb1; middle-sized triple-circled spheres, Rb2; largest spheres, Cl1; largest-hatched spheres, Cl2.

separations and lower absolute charges of these anions.

Thus, the maximum Madelung constant can be obtained first by changing the anion parameters which are coordinated to the highest valency cation. Because these anions are also coordinated to the lower valency cation, the second process would be the maximization of the Madelung constant by changing the atom parameters of the latter cation. The validity of this order means implicitly that the anion parameters are not sensitive to the parameters of the lower valency cations.

TABLE IV

MADELUNG CONSTANTS OF Rb_2PuCl_6 AS A FUNCTION OF PARAMETERS u(Cl1) AND u(Cl2) FOR Pu–Cl DISTANCE 2.57 Å[a]

	Parameter u(Cl1)		
Parameter u(Cl2)	0.155 (0.35005)[b]	0.156 (0.35209)	0.1565 (0.35308)
0.492 (0.11705)[c]	16.26920	16.26869	16.26821
0.494 (0.11985)	16.26993	16.26987	16.26961
0.496 (0.12276)	16.26980	16.27022	16.27019
0.498 (0.12577)	16.26881	16.26972	16.26994
0.500 (0.12890)	16.26701	16.26844	16.26891
u(Cl2) which gives maximal Madelung constant[d]	0.49480	0.49585	0.49660
Maximal Madelung constant[d]	16.27005	16.27022	16.27022

[a] Rubidium parameters are those for β-Rb_2GeF_6, i.e., u(Rb1) = 0.8440 and u(Rb2) = 0.5867.

[b] Values in parentheses: v(Cl1).

[c] Values in parentheses: v(Cl2).

[d] Graphically determined.

In Rb_2PuCl_6, three Cl1 anions and three Cl2 anions are coordinated around Pu^{4+}. Calculation was made starting from the use of the atom parameters of β-Rb_2GeF_6 (*18*), viz. u(Rb1) = 0.8440, u(Rb2) = 0.5867, u(Pu) = 0.25, u(Cl1) = 0.1657, v(Cl1) = 0.3367, u(Cl2) = 0.4691, and v(Cl2) = 0.1138. First, u(Cl1) was changed around 0.1657, and v(Cl1) which gave the maximum Madelung constant was obtained by graphical interpolation for each u(Cl1). According to the result, such v(Cl1) values were those which gave rise to the Pu–Cl distance equal to the Pu–Cl2 distance (2.372 Å) defined by u(Cl2) and v(Cl2), as had already been seen for β-Rb_2GeF_6 (*18*). Since v parameter is fixed by u parameter for a given Pu–Cl distance, if the relationship above holds, we can reduce two variables to be determined, i.e., v(Cl1) and v(Cl2).

We use as the critical distances the 0.1 Å smaller values than the sum of the crystal radii of Shannon (*24*). The critical distances for Rb–Cl, Pu–Cl, and Cl–Cl are 3.43, 2.57, and 3.24 Å, respectively, since the crystal radii of Rb^+ (coordination number (CN) = 12), Pu^{4+} (CN = 6), and Cl^- are 1.86, 1.00, and 1.67 Å, respectively. The atom parameters of β-Rb_2GeF_6 result in the Pu–Cl distance of 2.372 Å which is less than the critical distance, 2.57 Å. Therefore, maximization of the Madelung constant was next carried out under the condition of L(=Pu–Cl) = 2.57 Å. As stated above, this was done by changing functionally the u(Cl1) and u(Cl2) parameters. Table IV lists the variation of the Madelung constant with u(Cl1) and u(Cl2). For each of the u(Cl1) values, one can obtain the u(Cl1) value which gives the maximal Madelung constant. This u(Cl2) value and the maximal Madelung constant graphically determined are shown on the lower two lines of the table. By another graphical analysis, it was found that the maximum of the maximal Madelung constants (16.27023) was obtained at u(Cl1) = 0.15625 and u(Cl2) = 0.49610 (and, therefore, at v(Cl1) = 0.35259 and v(Cl2) = 0.12291). Inspection of atomic separations, however, revealed that Rb1–Cl2 = 3.413 and Rb2–Cl1 = 3.424 Å with these chlorine parameters. In order to increase these separations to the critical distance, 3.43 Å, the atom parameters of rubidium had to be changed to u(Rb1) = 0.89331 and u(Rb2) = 0.58736, which gave the Madelung constant 16.24573 (maximum of $|h|$, $|k|$, and $|l|$ = 12). This Madelung con-

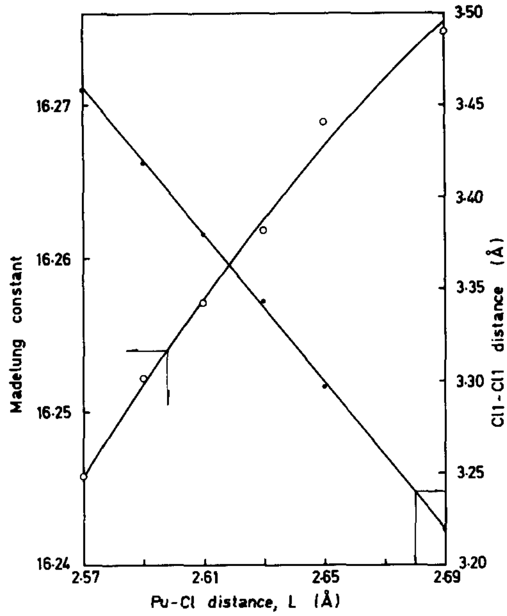

FIG. 2. Change of the Madelung constant and the shortest Cl–Cl distance as a function of Pu–Cl distance, *L*, for Rb_2PuCl_6.

stant is smaller than the former value, 16.27023. From these results, it is seen that Conditions 1 and 2 are satisfied for $L = 2.57$ Å with the above parameters.

The same procedure was carried out for the other *L*'s. The results are shown in Fig. 2. It is seen from the figure that the Madelung constant increases with increasing *L*. This means that the crystal is more stable with larger *L*. However, the distances Rb1–Cl1, Rb2–Cl1, and Cl1–Cl1 decrease with increasing *L*. The rate of decrease is low for Rb1–Cl1 and Rb2–Cl1 distances. In the case of Rb1–Cl1, the distances are 3.722 and 3.712 Å for $L = 2.57$ and 2.69 Å, respectively, and for Rb2–Cl1, 3.713 and 3.578 Å for $L = 2.57$ and 2.69 Å, respectively. On the other hand, the Cl1–Cl1 distance decreases more rapidly. The shortest Cl–Cl distance is 3.458 Å for $L = 2.57$ Å, while it lowers to 3.219 Å for $L = 2.69$ Å. The latter is smaller than the critical distance of Cl–Cl (3.24 Å). Change of the Cl1–Cl1 distance with *L* is also depicted in Fig. 2, from which the *L* value corresponding to 3.24 Å is calculated to be 2.680 Å.

The maximization process was followed for $L = 2.680$ Å as had been done for $L = 2.57$ Å. The atom parameters obtained are $u(\mathrm{Rb1}) = 0.8805$, $u(\mathrm{Rb2}) = 0.5943$, $u(\mathrm{Cl1}) = 0.1464$, $v(\mathrm{Cl1}) = 0.3523$, $u(\mathrm{Cl2}) = 0.4972$, and $v(\mathrm{Cl2}) = 0.1092$ with the presentation of the values to 10^{-4} decimal units (Table III). The Madelung constant is 16.27270 with *h*, *k*, and *l*'s from −16 to 16. The Madelung energy is −2019.05 kcal/mol. In column 5 of Table II, the intensities of diffraction peaks calculated for the above parameters by means of LAZY-PULVERIX program of which atomic scattering factors are those from "International Tables for X-ray Crystallography" (*25*) are given. These *I*(calc) are seen to be in good agreement with respective *I*(obs). Table V shows bond distances and angles for this compound.

The diffraction pattern of K_2PuCl_6 was quite different from that of Rb_2PuCl_6. Attempts to assign the diffraction lines to tetragonal, hexagonal, or orthorhombic systems were all unsuccessful. The possibility of a mixture of cubic and hexagonal phases was also rejected because of unsatisfactory

TABLE V

BOND DISTANCES (Å) AND ANGLES (°) FOR Rb_2PuCl_6[a]

Pu–Cl1	2.680(3×)	Cl1–Cl1	3.240(2×)
Pu–Cl2	2.680(3×)	Cl1–Cl1	4.137(2×)
Cl1–Pu–Cl1	101.04	Cl1–Cl2	3.665(2×)
Cl1–Pu–Cl2	86.27	Cl2–Cl2	3.626(2×)
Cl2–Pu–Cl2	85.15	Cl2–Cl2	3.751(2×)
Rb1–Cl1	3.713(6×)	Rb2–Cl1	3.430(3×)
Rb1–Cl2	3.430(3×)	Rb2–Cl1	3.591(3×)
Rb1–Cl2	3.883(3×)	Rb2–Cl2	3.693(6×)
Cl1–Rb1–Cl1	51.74	Cl1–Rb2–Cl1	53.64
Cl1–Rb1–Cl1	67.72	Cl1–Rb2–Cl1	56.37
Cl1–Rb1–Cl2	57.64	Cl1–Rb2–Cl2	60.40
Cl1–Rb1–Cl2	64.37	Cl1–Rb2–Cl2	64.59
Cl1–Rb1–Cl2	83.47	Cl1–Rb2–Cl2	87.95
Cl2–Rb1–Cl2	57.76	Cl2–Rb2–Cl2	58.81
Cl2–Rb1–Cl2	63.83	Cl2–Rb2–Cl2	61.04

[a] Final significant figures are given for comparative purposes; precision is ca. ± 0.01 Å or 0.1°.

TABLE VI

Observed and Calculated Q Values and Intensities for K_2PuCl_6

(*hkl*)	Q(obs)[a]	Q(calc)	I(obs)[b]	I(calc)
011	0.0273	0.0269	10	10
$10\bar{1}$	0.0284	0.0281	6	9.0
101	0.0299	0.0296	7	7.3
110	0.0369	0.0365	7	8.3
002	0.0389	0.0384	4	4.2
020	0.0701	0.0691	1	2.3
$11\bar{2}$	0.0740	0.0734	4	4.0
112	0.0771	0.0764	5	3.9
200		0.0768		2.1
$12\bar{1}$	0.0978	0.0971	3	2.8
121	0.0993	0.0986	2	2.3
$21\bar{1}$	0.1028	0.1022	5	2.5
$10\bar{3}$		0.1034		1.0
013	0.1043	0.1037	3	3.5
211		0.1052		2.4
022	0.1086	0.1075	3	0.4
103		0.1079		1.1
220	0.1467	0.1459	4	9.1
004	0.1545	0.1537	3	4.0
031	0.1663	0.1650	1	1.6
$12\bar{3}$	0.1735	0.1724	1	0.7
130	0.1750	0.1746	2bbb	1.2
$21\bar{3}$		0.1760		1.9
123	0.1774	0.1770		0.8
$30\bar{1}$	0.1819	0.1802	2b	0.5
$22\bar{2}$		0.1813		1.2
301	0.1859	0.1847	2	0.3
213		0.1851		1.8
$11\bar{4}$	0.1883	0.1871	2	1.3
222		0.1873		1.0
310	—	0.1901	—	1.1
114	0.1939	0.1932	1	1.2
$13\bar{2}$	—	0.2115	—	1.1
132	—	0.2145	—	1.1
024	0.2199	0.2227	1	0.9
$31\bar{2}$	0.2247	0.2240	2bb	1.0
$20\bar{4}$		0.2245		0.4
312	0.2342	0.2331	1	1.0
204	—	0.2365	—	0.4
$23\bar{1}$	—	0.2403	—	0.6
033	0.2424	0.2418	2	1.4
231		0.2433		0.6
$32\bar{1}$	0.2502	0.2493	<1	1.6
214	0.2537	0.2538	<1	1.1
$10\bar{5}$		0.2555		0.7
105	—	0.2631	—	0.6
040	—	0.2762	—	1.8
$22\bar{4}$	0.2948	0.2935	2	3.0
$14\bar{1}$	0.3068	0.3043	2b	0.9
224		0.3056		2.9
141		0.3058		0.7
400		0.3073		1.4
$23\bar{3}$	—	0.3141	—	0.7
042		0.3146		0.5
233	0.3260	0.3232	2bb	0.7
$12\bar{5}$		0.3246		0.8
$13\bar{4}$		0.3252		0.6
$21\bar{5}$		0.3267		0.3
330		0.3282		0.5
$41\bar{1}$	0.3320	0.3312	1	0.5
134		0.3313		0.6
125		0.3321		0.7
$31\bar{4}$	—	0.3348	—	0.6
323		0.3352		0.8
411	0.3369	0.3372	<1	0.4
402	0.3497	0.3518	1bbb	0.2
314		0.3529		0.5
240	0.3538	0.3531		0.6
420	0.3782	0.3764	2	0.6
$11\bar{6}$		0.3777		0.3
$14\bar{3}$		0.3796		0.4
116	0.3880	0.3867	<1	0.4
035	0.3962	0.3955	<1	0.3
$30\bar{5}$	0.4028	0.4017	<1	0.3
$41\bar{3}$		0.4020		0.6

[a] $Q = 1/d^2$ in $Å^{-2}$.

[b] Visually estimated.

agreement between observed and calculated Q's. Good agreement was observed when a monoclinic system was taken. Least-squares fitting with the Nelson–Riley method was carried out for the diffraction lines collected by the Guinier camera on the LCR-2 program in a similar way to that of Rb_2PuCl_6. This was done for the lines up to $Q = 0.4028$. The crystal data so determined are shown in Table I. The observed and calculated Q values are tabulated in Table VI for each of the (*hkl*) reflections.

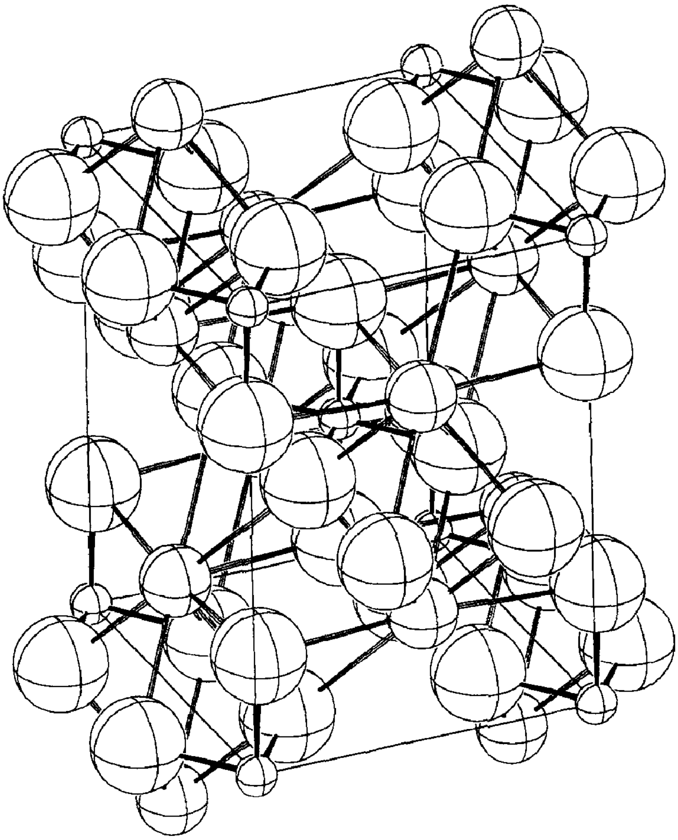

FIG. 3. Perspective view of K_2PuCl_6 which shows atomic arrangement in this crystal structure. Smallest spheres, Pu; middle-sized spheres, K; largest spheres, Cl.

The crystal structure of K_2PuCl_6 was found to be one slightly distorted from the cubic K_2PtCl_6 structure. With this and the fact that there were no conditions in (hkl) for reflections in mind, $P2/m$ was left as the space group which could consistently accommodate the K_2PtCl_6-type atomic arrangement. Figure 3 shows a perspective view of the K_2PuCl_6 crystal. Each plutonium atom is coordinated by 6 chlorine atoms forming an octahedron, and around each potassium atom there are 12 chlorine atoms.

The variable atom parameters were determined by means of the electrostatic calculations as in the case of Rb_2PuCl_6. For having the crystal structure of K_2PuCl_6, 14 variable atom parameters should be determined. Their symmetry relations are shown in Table VII. The ideal values of these parameters are: $x(\mathrm{K1}) = \frac{1}{2}$, $z(\mathrm{K1}) = \frac{1}{4}$, $x(\mathrm{K2}) = 0$, $z(\mathrm{K2}) = \frac{3}{4}$, $x(\mathrm{Cl1}) = 0$, $z(\mathrm{Cl1}) = \frac{1}{4}$, $x(\mathrm{Cl2}) = \frac{1}{2}$, $z(\mathrm{Cl2}) = \frac{3}{4}$, $x(\mathrm{Cl3}) = \frac{1}{4}$, $y(\mathrm{Cl3}) = \frac{1}{4}$, $z(\mathrm{Cl2}) = \frac{3}{4}$, $x(\mathrm{Cl3}) = \frac{1}{4}$, $y(\mathrm{Cl3}) = \frac{1}{4}$, $z(\mathrm{Cl3}) = 0$, $x(\mathrm{Cl4}) = \frac{3}{4}$, $y(\mathrm{Cl4}) = \frac{3}{4}$, and $z(\mathrm{Cl4}) = \frac{1}{2}$. Here, we assumed that the crystal is practically invariant against the translation $(\frac{1}{2}, \frac{1}{2}, \frac{1}{2})$. That is to say, the atom arrangement around Pu2 is the same as that around Pu1, which reduced the number of the variable atom parameters to seven with the following relations, viz. $x(\mathrm{K2}) = x(\mathrm{K1}) + \frac{1}{2}$, $z(\mathrm{K2})$

TABLE VII

Atom Positions in K_2PuCl_6 (Space Group $P2/m$)

K1:	(2m)	$x, 0, z; \bar{x}, 0, \bar{z}$ with $x = 0.4913$, $z = 0.2772$
K2:	(2n)	$x, \frac{1}{2}, z; \bar{x}, \frac{1}{2}, \bar{z}$ with $x = -0.0088$, $z = 0.7772$
Pu1:	(1a)	0, 0, 0
Pu2:	(1h)	$\frac{1}{2}, \frac{1}{2}, \frac{1}{2}$
Cl1:	(2m)	with $x = 0.0099$, $z = 0.2519$
Cl2:	(2n)	with $x = 0.5099$, $z = 0.7519$
Cl3:	(4o)	$x, y, z; \bar{x}, y, \bar{z}; \bar{x}, \bar{y}, \bar{z}; x, \bar{y}, z$ with $x = 0.2278$, $y = 0.2595$, $z = 0.0000$
Cl4:	(4o)	with $x = 0.7278$, $y = 0.7595$, $z = 0.5000$

$= z(\mathrm{K1}) + \frac{1}{2}$, $x(\mathrm{Cl2}) = x(\mathrm{Cl1}) + \frac{1}{2}$, $z(\mathrm{Cl2}) = z(\mathrm{Cl1}) + \frac{1}{2}$, $x(\mathrm{Cl4}) = x(\mathrm{Cl3}) + \frac{1}{2}$, $y(\mathrm{Cl4}) = y(\mathrm{Cl3}) + \frac{1}{2}$, and $z(\mathrm{Cl4}) = z(\mathrm{Cl3}) + \frac{1}{2}$.

The next problem is whether it is true also for K_2PuCl_6 that all the Pu–Cl bond lengths are the same. Since each Pu1 atom is surrounded by two Cl1 and four Cl3 atoms, and each Pu2 atom by two Cl2 and four Cl4 atoms in this crystal, this was checked by changing the $x(\mathrm{Cl3})$ parameter and finding the point which gave the maximum of Madelung constant for a fixed set of the parameters, $x(\mathrm{Cl1})$, $z(\mathrm{Cl1})$, $y(\mathrm{Cl3})$, and $z(\mathrm{Cl3})$. The result showed that such a $x(\mathrm{Cl3})$ parameter brought about the Pu1–Cl3 distance the same as the Pu1–Cl1 distance. Therefore, $x(\mathrm{Cl3})$ can be determined as a function of $y(\mathrm{Cl3})$ and $z(\mathrm{Cl3})$ for a given L (one more variable was reduced).

The critical distances in this coordination for K–Cl, Pu–Cl, and Cl–Cl are 3.35, 2.57, and 3.24 Å, respectively, because K^+(CN = 12) is 1.78 Å (*24*). Then, we performed calculations starting from $L = 2.57$ Å. For doing this, it was first assumed that the two apical Pu1–Cl1 bonds were in the direction perpendicular to the (001) plane, which gave $x(\mathrm{Cl1}) = 0.00988$, $z(\mathrm{Cl1}) = 0.25186$, $x(\mathrm{Cl2}) = 0.50988$, and $z(\mathrm{Cl1}) = 0.75186$ for $L = 2.57$ Å directly without Madelung constant calculation. The Madelung constants were computed for several sets of $x(\mathrm{Cl3})$ and $y(\mathrm{Cl3})$ parameters that yield the Pu1–Cl3 distance of 2.57 Å together with the above Cl1 and Cl2 parameters leaving the other parameters at the ideal values. Table VIII shows the change of the constants. By graphical interpolation of these values, it is seen that the maximum of the maximal Madelung constants, 15.93476, is obtained at $x(\mathrm{Cl3}) = 0.22782$ and $y(\mathrm{Cl3}) = 0.25950$. However, the K2–Cl3 distances are less than the critical distance 3.35 Å with these parameter values. Therefore, calculation of the Madelung constants and atomic separations were made for various pairs of $x(\mathrm{K2})$ and $z(\mathrm{K2})$ with the aim of finding the K2 parameters which would give the maximum Madelung constant under the restriction K2–Cl3 $\geqq$ 3.35 Å. The maximum Madelung constant was obtained at $x(\mathrm{K2}) = -0.00875$ and $z(\mathrm{K2}) = 0.77722$ which gave four K2–Cl3 distances, all of 3.35 Å. The Madelung constant with the above Cl3 and K2 parameters together with the corresponding Cl4 and K1 parameters, i.e., $x(\mathrm{Cl4}) = 0.72782$, $y(\mathrm{Cl4}) = 0.7595$, $z(\mathrm{Cl4}) = 0.5$, $x(\mathrm{K1}) = 0.49125$, and $z(\mathrm{K1}) = 0.27722$, was calcu-

TABLE VIII

Change of Maximal Madelung Constants of K_2PuCl_6 for Several Sets of $x(\mathrm{Cl3})$ and $y(\mathrm{Cl3})$ Parameters which are to Produce Pu1–Cl3 Distance 2.57 Å[a]

$x(\mathrm{Cl3})$	$y(\mathrm{Cl3})$	Madelung constant
0.22971	0.2580	15.93466
0.22908	0.2585	15.93471
0.22845	0.2590	15.93475
0.22782	0.2595	15.93476
0.22718	0.2600	15.93475
0.22655	0.2605	15.93472
0.22591	0.2610	15.93467

[a] Apical Pu1–Cl1 bonds have a separation 2.57 Å and are perpendicular to the (001) plane. Corresponding parameters are: $x(\mathrm{Cl1}) = 0.00988$, $z(\mathrm{Cl1}) = 0.25186$, $x(\mathrm{Cl2}) = 0.50988$, and $z(\mathrm{Cl2}) = 0.75186$. Other parameters are put to the ideal positions.

TABLE IX

BOND DISTANCES (Å) AND ANGLES (°) FOR K_2PuCl_6[a]

Pu1–Cl1	2.570(2×)	Pu2–Cl2	2.570(2×)
Pu1–Cl3	2.570(4×)	Pu2–Cl4	2.570(4×)
Cl3–Pu1–Cl3	79.56	Cl4–Pu2–Cl4	79.56
Cl3–Pu1–Cl3	100.44	Cl4–Pu2–Cl4	100.44
Cl3–Pu1–Cl3	180.00	Cl4–Pu2–Cl4	180.00
Cl1–Pu1–Cl3	90.00	Cl2–Pu2–Cl4	90.00
K1–Cl4	3.350(4×)	K2–Cl3	3.350(4×)
K1–Cl1	3.477(1×)	K2–Cl2	3.477(1×)
K1–Cl1	3.760(1×)	K2–Cl2	3.760(1×)
K1–Cl2	3.817(2×)	K2–Cl1	3.817(2×)
K1–Cl3	3.902(2×)	K2–Cl4	3.902(2×)
K1–Cl3	4.042(2×)	K2–Cl4	4.042(2×)
Cl3–Cl3	3.289(1×)	Cl4–Cl4	3.289(1×)
Cl3–Cl2	3.617(1×)	Cl4–Cl1	3.617(1×)
Cl3–Cl1	3.635(2×)	Cl4–Cl2	3.635(2×)
Cl3–Cl3	3.661(1×)	Cl4–Cl4	3.661(1×)
Cl3–Cl2	3.768(1×)	Cl4–Cl1	3.768(1×)
Cl3–Cl3	3.929(1×)	Cl4–Cl4	3.929(1×)
Cl3–Cl3	3.950(1×)	Cl4–Cl4	3.950(1×)
Cl3–Cl3	4.921(1×)	Cl4–Cl4	4.921(1×)

[a] See footnote to Table V.

lated to be 15.94772 (max of $|h|$, $|k|$, $|l|$ = 16).

Calculation for L = 2.59 and 2.61 Å was carried out in the same way. The Madelung constants obtained were 15.93331 and 15.86820, respectively. The constant decreases monotonously with increasing L, which indicates that the atom arrangement with L = 2.57 Å is the most stable.

The above calculations were made on the assumption that the direction of the Pu1–Cl1 bonds and, therefore, that of the Pu2–Cl2 bonds are perpendicular to the (001) plane. To examine the appropriateness of this assumption, the Madelung constants were maximized for the two cases of L = 2.57 Å, i.e., 89.59 and 90.79°. The maximum Madelung constants under the condition K–Cl = 3.35 Å were calculated to be 15.92537 and 15.92425, respectively. Because these values are smaller than that for the 90° case, 15.94776, *tilting of the octahedra with respect to the direction perpendicular to the (001) plane is electrostatically unfavorable.*

Another point which should be examined is the possibility of the difference in the atomic arrangements around Pu1 and Pu2. Calculation was performed for the case that the direction of the Pu1–Cl1 bonds was 89.59° while that of the Pu2–Cl2 bonds was 90° in the same crystal. The maximum Madelung constant with the above set of atom parameters was 15.93765 which was also smaller than 15.94772.

Consequently, the most reasonable atom parameters for K_2PuCl_6 are those listed in Table VII. The corresponding Madelung constant is 15.94772. The Madelung energy is −2063.50 kcal/mol. The intensities of diffraction peaks calculated using these parameters are shown in column 5 of Table VI. As seen from the table, these I(calc) accord well with the I(obs). Table IX shows bond distances and angles for this compound.

Discussion of the Structures

Figures 4a and 4b show the Raman spectra of Rb_2PuCl_6 and K_2PuCl_6, respectively. If $PuCl_6^{2-}$ in these compounds has cubic O_h site symmetry, the Raman-active modes should be nondegenerate $\nu_1(A_{1g})$, twofold degenerate $\nu_2(E_g)$, and threefold degenerate $\nu_5(F_{2g})$. However, in the case of lower symmetry (D_{3d}, D_{2h}), the degenerate Raman-active lines should be split into two or more lines. The $PuCl_6^{2-}$ symmetry is not regularly octahedral in both Rb_2PuCl_6 and K_2PuCl_6. As a quantitative measure of distortion, the angle Cl–Pu–Cl can be used. If all Pu–Cl distances were the same and all Cl–Pu–Cl angles were 90°, the point group would be O_h. The angles are 101.04, 86.27, and 85.15° for Rb_2PuCl_6 (Table V) and are 100.44, 90.00, and 79.56° for K_2PuCl_6 (Table IX). As the result, a slight broadening of the ν_5 lines at 132 cm^{-1} is observed in Fig. 4 with respect to the nondegenerate ν_1 (312 and 307 cm^{-1} for Rb_2PuCl_6 and K_2PuCl_6, respectively) lines, whereas existence of shoulders is unclear. There have been reports on infrared and Raman spectra for α-

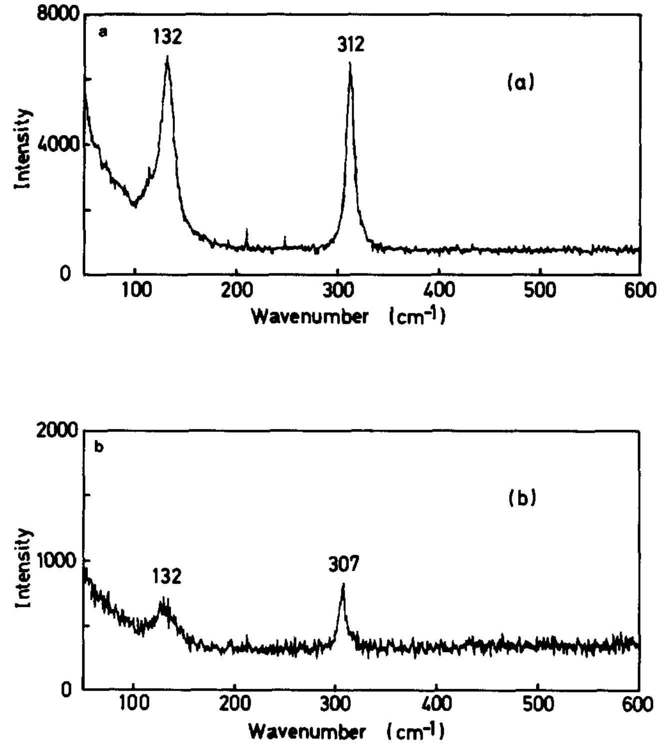

FIG. 4. Raman spectra for Rb_2PuCl_6 and K_2PuCl_6. (a) Rb_2PuCl_6. (b) K_2PuCl_6.

Cs_2UCl_6 (*26, 27*) which crystallizes in the trigonal system with space group $P\bar{3}m1$. The site symmetry, $AnCl_6^{2-}$, is D_{3d} and is significantly different from O_h for Cs_2UCl_6 since the angles Cl–U–Cl are calculated to be 94.57 and 85.43° using the reported atom parameters (*13*). Shamir and Silberstein (*26*) observed the Raman spectra for α-Cs_2UCl_6 at $\nu_1 = 308$ and $\nu_5 = 126$ cm^{-1} which are in good agreement with $\nu_1 = 307$ and $\nu_5 = 125$ by Brown *et al.* (*27*). They do not report any indication of structure in the ν_5 spectra. Such insensitivity to distortion may be explained by taking into account the effect of lighter alkali metals in the compounds as Berringer *et al.* (*28*) claimed.

The Raman positions for Cs_2NpCl_6 and Cs_2PuCl_6, both having the same crystal structure as α-Cs_2UCl_6, are $\nu_1 = 310$, $\nu_5 = 128$ cm^{-1} and $\nu_1 = 309$, $\nu_5 = 129$ cm^{-1}, respectively. It is seen that these compounds, including the present compounds, show nearly the same Raman spectra. The ν_2 lines were not observed for either Rb_2PuCl_6 or K_2PuCl_6, which is consistent with the results of Brown *et al.* (*27*) for several hexahalogeno complexes.

The crystal structure of Rb_2PuCl_6 ($P6_3mc$, β-Rb_2GeF_6-type structure) is the same as Cs_2BkCl_6 (*15*). The *c* axis of the Rb_2PuCl_6 crystal is twice as long as the *c* axis of the Cs_2PuCl_6 structure ($P\bar{3}m1$, α-Rb_2GeF_6-type structure), with alternate layers rotated 180° about sixfold screw axes. As seen in Fig. 1, the layers of $Cs^+ + Cl^-$ ions form close-packed "planes" and Pu^{4+} ions fill alternate octahedral interstices formed by six Cl^- ions. In the case of Cs_2PuCl_6, the arrangement of the layers corresponds to hexagonal close packing, ABABAB, while it corresponds to double-hexagonal close packing, ABACABAC, for Rb_2PuCl_6. A crystal of ideally hexagonally close-packed spheres has $c/a = 1.633$. Since all atoms are not identical in Rb_2PuCl_6 and the unit cell base has a length double that of hexagonally close-packed metals, the c/a ratio for Rb_2PuCl_6 is 1.610 which is not far from the ideal value and a little smaller than that of Cs_2BkCl_6 (1.624). As mentioned before, the octahedra formed by the six Cl^- ions are slightly deformed from the regular octahedra although six Pu–Cl distances are all the same. It is noteworthy that this distance, 2.680 Å, is longer than the critical distance, 2.57 Å, by 0.11 Å which is in contrast to the case of K_2PuCl_6 where the distance is 2.57 Å. Since only a c/a ratio concerns the atom parameters in the electrostatic calculations used in this paper, this longer distance may be caused by its particular c/a ratio and/or the longer dimensions of the unit cell edges.

K_2PuCl_6 has the crystal structure of distorted K_2PtCl_6 type (cubic, $Fm3m$). Its relationship to the ideal K_2PtCl_6 structure can easily be seen by choosing new axes of reference a' and b' in the direction [110] and [$1\bar{1}0$], respectively. The cell edges of a' and b' are both $(a^2 + b^2)^{1/2} = 10.485$ Å which is slightly larger than c (10.208 Å). The angle between a' and b' is 93.092°. The octahedron around a Pu1 atom consists of four Cl3 and two Cl1 atoms, while that around a Pu2 atom is four Cl4 and two Cl2 atoms. These two octahedra are the same in shape but the position of their location is different, Pu2 being in ($\frac{1}{2}$, $\frac{1}{2}$, $\frac{1}{2}$) position. These are not regular though all the Pu–Cl distances are the same and equal to 2.57 Å. The Pu1 atom at origin and the four Cl3 atoms coordinated to it are within a sheet parallel to (001) plane. The Cl3 atoms are apart from Pu1 1.6427 and 1.9751 Å in the directions of a and b axes, respectively. Therefore, their arrangement is rectanglar if projected on (001). The angle Cl3–Pu1–Cl3 with respect to the neighboring Cl3 atoms is either 100.44 or 79.56°. It is interesting that the octahedra undergo a distortion larger than the cell itself. Two Pu1–Cl1 bonds to the same Pu1 are in a straight line perpendicular to the plane formed by the four Cl3 atoms.

We see that Cs_2PuCl_6, Rb_2PuCl_6, and K_2PuCl_6 crystallize in trigonal $P\bar{3}m1$, hexagonal $P6_3mc$, and monoclinic $P2/m$ structures, respectively. It is evident that the alkali metals are responsible for these different crystal structures. In the compounds, Cs_2PuCl_6 is the most stable which can be prepared from aqueous solutions (*29*). K_2PuCl_6 appears to be less stable than Rb_2PuCl_6. The weaker Raman spectra of K_2PuCl_6 (Fig. 4b) may be due to partial decomposition of this compound during exposure to the laser beam. The order of stability will be

$$Cs_2PuCl_6 > Rb_2PuCl_6 > K_2PuCl_6.$$

Let us discuss briefly the relative stability of Cs_2PuCl_6 and Rb_2PuCl_6 structures by means of electrostatic calculations. If there exists imaginary i-Rb_2PuCl_6 which has the Cs_2PuCl_6-type structure with lattice constants $a(i\text{-}Rb_2PuCl_6) = a(Rb_2PuCl_6) = 7.377$ Å and $c(i\text{-}Rb_2PuCl_6) = c/2(Rb_2PuCl_6) = 5.940$ Å, the calculation shows that the maximum stability of the crystal would be attained with the atom parameters $u(Rb) = 0.7124$, $u(Cl) = 0.1767$, and $v(Cl) = 0.2424$ where $u(Rb)$ is the parameter of rubidium atoms in the (2d) position of space group $P\bar{3}m1$, and $u(Cl)$ as well as $v(Cl)$ are those of chlorine atoms in the (6i) position (*12*). The Madelung constant 16.37981 yields the Madelung energy −2031.51 kcal/mol with these atom parameters. This value of energy is lower than that of Rb_2PuCl_6 really existing with the β-Rb_2GeF_6-type structure. It seems, however, that the lattice dimensions for i-Rb_2PuCl_6 ought to be shortened. In fact, in the case of Rb_2GeF_6 which has both of the modifications, i.e., α-Rb_2GeF_6 ($P\bar{3}m1$, low temperature form) and β-Rb_2GeF_6 ($P6_3mc$, high-temperature form), the lattice constants for α-Rb_2GeF_6 are $a = 5.82$ and $c = 4.79$ Å (*30*), while those for β-Rb_2GeF_6 are $a = 5.94$ and $c = 9.63$ Å (*12*); $c/2$ of β-Rb_2GeF_6 is 4.815 Å, which is also larger than the c edge of α-Rb_2GeF_6. As a crude approximation, let the lattice parameter ratio of *i*-Rb_2PuCl_6 and Rb_2PuCl_6 be the same as that of α- and β-Rb_2GeF_6. Using the lattice parameters of Rb_2PuCl_6, those of *i*-Rb_2PuCl_6 are calculated to be $a = 7.228$ and $c = 5.909$ Å.

The electrostatic calculation was carried out in order to have the variable atom parameters for these lattice constants. The result is $u(\mathrm{Rb}) = 0.7725$, $u(\mathrm{Cl}) = 0.1847$, and $v(\mathrm{Cl}) = 0.2848$ which give the Madelung constant and energy, 16.15641 and −1878.99 kcal/mol, respectively. It is seen that the Madelung energy for *i*-Rb_2PuCl_6 is higher than that of Rb_2PuCl_6. Also, the shortest Cl–Cl distance with the above parameters, 3.224 Å, is less than the critical distance of Cl–Cl, viz. 3.24 Å. If the Cl–Cl distance is elongated to 3.24 Å by changing $u(\mathrm{Cl})$ and $v(\mathrm{Cl})$, the Madelung constant decreases still farther. The main reason of instability of *i*-Rb_2PuCl_6 may be the longer Pu–Cl separations (2.859 Å). Due to smaller crystal radius of Rb^+(CN = 12) as compared with Cs^+, the unit cell contracts to a greater degree in a than c, which might reduce significantly the stability of the *i*-Rb_2PuCl_6 until it cannot exist as a real crystal.

Acknowledgments

The authors are grateful to Dr. L. Stein who kindly took the Raman spectra. They also thank Dr. W. T. Carnall for helpful discussions during the course of this work. The work reported herein was performed under the auspices of the Office of Basic Energy Sciences, Division of Chemical Sciences, U.S. Department of Energy, under Contract W-31-109-ENG-38.

References

1. W. H. Zachariasen, *Acta Crystallogr.* **2,** 388 (1949).
2. W. H. Zachariasen, *J. Amer. Chem. Soc.* **70,** 2147 (1948).
3. G. Brunton, *Acta Crystallogr. B* **25,** 2163 (1969).
4. L. A. Harris, *Acta Crystallogr.* **13,** 502 (1960).
5. A. Cousson, A. Tabuteau, M. Pagès, and M. Gasperin, *Acta Crystallogr. B* **35,** 1198 (1979).
6. C. Keller and H. Schmutz, *Inorg. Nucl. Chem. Lett.* **2,** 353 (1966).
7. I. F. Alenchikova, L. L. Zaitseva, L. V. Lipis, V. V. Fomin, and N. T. Chebotarev, *Proc. Int. Conf. Peaceful Uses At. Energy 2nd* **28,** 309 (1958).
8. W. H. Zachariasen, *Acta Crystallogr.* **1,** 265 (1948).
9. F. H. Kruse, *J. Inorg. Nucl. Chem.* **33,** 1625 (1971).
10. T. K. Keenan, *Inorg. Nucl. Chem. Lett.* **3,** 463 (1967).
11. V. M. Vdovenko, V. A. Volkov, I. I. Kozhina, and I. G. Suglobova, *Sov. Radiochem.* **14,** 492 (1972).
12. W. G. Wyckoff, "Crystal Structures," Vol. 3, Chap. IX-C, Interscience, New York (1965).
13. S. Siegel, *Acta Crystallogr.* **9,** 827 (1956).
14. W. H. Zachariasen, *Acta Crystallogr.* **1,** 268 (1948).
15. L. R. Morss and J. Fuger, *Inorg. Chem.* **8,** 1433 (1969).
16. V. M. Vdovenko, V. A. Volkov, I. I. Kozhina, and I. G. Suglobova, *Sov. Radiochem.* **14,** 489 (1972).
17. P. J. Bendall, A. N. Fitch, and B. E. F. Fender, *J. Appl. Crystallogr.* **16,** 164 (1983).
18. T. Fujino and L. R. Morss, *J. Solid State Chem.* **67,** 131 (1987).
19. D. Cohen, *J. Inorg. Nucl. Chem.* **18,** 211 (1961).
20. D. E. Williams, "Ames Laboratory Report IS-1052," Iowa State University (1964).
21. E. F. Bertaut, *J. Phys. Radium* **13,** 499 (1952).
22. H. D. B. Jenkins and K. F. Pratt, *Chem. Phys. Lett.* **62,** 416 (1979).
23. Q. C. Johnson and D. H. Templeton, *J. Chem. Phys.* **34,** 2004 (1961).
24. R. D. Shannon, *Acta Crystallogr. A* **32,** 751 (1976).
25. "International Tables for X-Ray Crystallography," Vol. IV, Kynoch Press, Birmingham, England (1974).
26. J. Shamir and A. Silberstein, *J. Inorg. Nucl. Chem.* **37,** 1173 (1975).
27. D. Brown, B. Whittaker, and P. E. Lidster, AERE-R 8035 (1975).
28. B. W. Berringer, J. B. Gruber, T. M. Loehr, and G. P. O'Leary, *J. Chem. Phys.* **55,** 4608 (1971).
29. J. Kooi, E. Weisskopf, and D. M. Gruen, *J. Inorg. Nucl. Chem.* **13,** 310 (1960).
30. W. B. Vincent and J. L. Hoard, *J. Amer. Chem. Soc.* **64,** 1233 (1942).